

Types of Discontinuous Percolation Transitions in Cluster Merging Processes

Y.S. Cho and B. Kahng

Department of Physics and Astronomy, Seoul National University 151-747, Korea

Recently, interest in discontinuous percolation transitions (DPTs) in cluster merging (CM) processes has been boosted as models for rapid spreading of epidemic diseases and opinion formation. Here we show that DPTs can be classified into two types, denoted as type I and type II, depending on the nature of the DPT. For the type I (type II), the transition occurs at unity (a finite threshold less than unity), and the order parameter increases drastically up to unity (a finite value less than unity and then does gradually). We study the origins of each type of DPT and present the necessary conditions for them. Moreover, we introduce a solvable model composed of two species of nodes, which leads to the point that the symmetric preserving (breaking) kinetics in the CM processes can be a key ingredient of the DPT of type I (type II).

PACS numbers: 64.60.ah,02.50.Ey,89.75.Hc

Percolation transition [1] (PT), the emergence of a macroscopic-scale cluster at a finite threshold, has played a central role as a model for metal-insulator and sol-gel [2] transitions in physical systems as well as the spread of disease epidemics [3] and opinion formation in complex systems. The ordinary percolation model and many models modified from it exhibit continuous transitions as a function of increasing occupation probability. Recently, however, a great interest in discontinuous percolation transitions (DPTs) has been sparked by the explosive percolation model [4], and the cascading-failure model in interdependent networks [5] because of their potential applications to real-world phenomena such as large-scale blackout in power-grid systems and the pandemic [6]. The explosive percolation model was an attempt to generate a DPT in cluster merging (CM) processes [4, 7–11], in which clusters are formed as links are added between two unconnected nodes following a given rule. However, recent extensive research works [12–15] show that the explosive percolation transition in random graph is continuous in the thermodynamic limit. This result has reinforced the robustness of continuous PTs in CM processes.

In order to induce a DPT in CM processes, we proposed an avoiding-a-spanning cluster (ASC) model [16] in Euclidean space. This model was successful to generate a DPT at a state in which all bonds of the systems are occupied in the thermodynamic limit. The order parameter $G(t)$, which is the fraction of nodes belonging to the largest cluster, increases drastically all the way to unity at the transition point. Moreover, such a pattern can be observed in other models such as a random aggregation model following the Smoluchowski coagulation equation [17], and the Gaussian model [18], etc. We denote this type of DPT as type-I DPT. Meanwhile, along with extensive studies on explosive percolation, a limited number of mathematical models [19–21] shows a different type of a DPT: the order parameter drastically increases at a finite threshold to a non-zero value that is less than unity, after which it gradually increases to unity. We denote such a transition as type-II DPT. However, models showing the type-II DPTs are rarely known,

although such type-II DPTs are more interesting than type-I DPTs because not only its origin is non-trivial in theoretical perspective but also similar behaviors appear in the k -core percolation [22, 23], discontinuous synchronization [24] and jamming [25] transitions.

Here, we show that the origins of two types of DPTs are different from each other. To uncover those origins, we examine the cluster size distributions at immediately before and after the percolation threshold, denoted as t_c^- and t_c^+ , where t is called time, defined as the number of links added to the system divided by system size N . To induce a type-II DPT, it is necessary that the clusters at t_c^- are heterogeneous in size, ranging from small cluster sizes to large ones. Among those clusters, large-size clusters primarily merge to create a macroscopic-scale giant cluster during a short time interval $[t_c^-, t_c^+]$. Beyond t_c^+ , the merging is mostly caused by remnant small-size clusters, of which number is $O(N)$, mainly joining the giant cluster. On the other hand, for a type-I DPT, at t_c^- , the remaining clusters are mainly of mesoscopic-scale size, which then merge during the interval $[t_c^-, t_c^+]$ to create a macroscopic-scale giant cluster. The details are discussed below.

We propose the necessary conditions for each type of DPT as follows: Here $n_s(t)$ denotes the number of s -size clusters divided by N , which changes with time.

- I) Necessary condition for a type-II DPT: At t_c^- , at least one characteristic cluster size $s^* > 1$ has to exist, which fulfills the following conditions in the thermodynamic limit: I-i) $\sum_{s=s^*}^{\infty} n_s(t_c^-) \rightarrow 0$, I-ii) $\sum_{s=1}^{\infty} n_s(t_c^-) \sim O(1)$, and I-iii) $\sum_{s=s^*}^{\infty} s n_s(t_c^-) = r$ ($0 < r < 1$).
- II) Necessary condition for a type-I DPT: At t_c^- , at least one characteristic cluster size $s^* > 0$ has to exist, which fulfills the following conditions in the thermodynamic limit: I-i) $\sum_{s=s^*}^{\infty} n_s(t_c^-) \rightarrow 0$, and II-ii) $\sum_{s=s^*}^{\infty} s n_s(t_c^-) = 1$.

To derive the necessary conditions, we suppose the extreme case that cluster aggregation dynamics occurs between clusters only of the size $s > s^*$ during a short time

interval between $[t_c^-, t_c^+]$. In this case, when inter-cluster links are added, the order parameter can increase the most rapidly. The number of links to connect all those clusters divided by N is $\sum_{s=s^*}^{\infty} n_s(t_c^-)$, which is equivalent to $\Delta t \equiv t_c^+ - t_c^-$.

First, we consider the case of a type-II DPT. To verify the condition I-i), we use the fact that if $\sum_{s=s^*}^{\infty} n_s(t_c^-) \rightarrow 0$ in the limit $N \rightarrow \infty$, then $\Delta t \rightarrow 0$. During this interval, since the order parameter increases as much as $O(1)$, the PT is discontinuous. Thus the condition I-i) provides a necessary condition for a discontinuous PT. To verify the condition I-ii), we consider the inequality $1 - \sum_{s=1}^{\infty} n_s(t_c^-) \leq t_c^-$, which comes from the fact that the number of links added up to t_c^- is larger than (or equal to) the number of cluster merging events. The equality holds when the model disallows the attachment of intra-cluster links. In general, when $\sum_{s=1}^{\infty} n_s(t_c^-)$ goes to zero, $t_c^- \geq 1$ in the thermodynamic limit. The condition I-ii) $\lim_{N \rightarrow \infty} \sum_{s=1}^{\infty} n_s(t_c^-) \sim O(1)$ provides a necessary condition that the transition point can be $t_c^- < 1$. Next, let us define $r = \sum_{s=s^*}^{\infty} s n_s(t_c^-)$, which corresponds to the size of powder keg in [9]. Then, $r = 1 - \sum_{s=1}^{s^*-1} s n_s(t_c^-)$. This quantity satisfies the following inequality. $r \leq 1 - \sum_{s=1}^{s^*-1} n_s(t_c^-) = 1 - \sum_{s=1}^{\infty} n_s(t_c^-) + \sum_{s=s^*}^{\infty} n_s(t_c^-)$. When the conditions I-i) and I-ii) hold, $r \leq 1 - O(1)$. Thus, $r < 1$. The condition I-iii) is needed to exclude the case $r = 0$ of a continuous transition. Thus, all the conditions I-i), I-ii), and I-iii) are needed for a type-II DPT.

We consider the case of a type-I DPT. Condition I-i) suggests that $\Delta t \rightarrow 0$ in the thermodynamic limit. Condition II-ii) suggests that $G(t_c^+) = 1$. Then using the inequality $1 - \sum_{s=1}^{\infty} n_s(t_c^-) \leq t_c^-$, one can obtain $t_c^- \geq 1$ in the thermodynamic limit. Thus the percolation threshold is positioned at $t_c \geq 1$. We remark that this necessary condition for a type-I DPT in a CM process is equivalent to $\lim_{N \rightarrow \infty} \sum_{s=1}^{\infty} n_s(t_c^-) = 0$.

In fact, our derivation is similar to the picture proposed by Friedman *et al.* [9] that whether the abrupt percolation transition taking place or not is determined by the number of the clusters in the powder keg region $s > s^*$. They set the characteristic size as $s^* \sim N^{1-\beta}$ with $\beta < 1$. Then, $\Delta t < N^{\beta-1}$ which is reduced to zero in the limit $N \rightarrow \infty$. This criterion is the same as the condition I-i). On the other hand, the authors of [9] did not concern the necessary conditions for a type-I or II DPT. In a similar way, Hooyberghs *et al.* [10] proposed another criterion for a DPT, which is again equivalent to our necessary condition for a type-I DPT.

Next, we introduce a cluster aggregation model that exhibits both a type-I and II DPT as a parameter changes. The dynamic rule is depicted schematically in Fig. 1. For this model, which is referred to as the two-species cluster aggregation (TCA) model, we start with N isolated nodes, half of which are colored black and the other half white. Color may represent opinion, for example, the left and the right wing position in a political issue. According to the dynamic rule below, all nodes

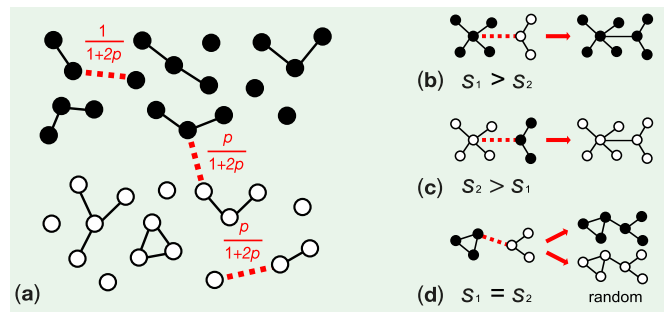


FIG. 1. (Color online) (a) There are three types of aggregations, each of which depends on the species of aggregating clusters. Probabilities for each case are given in the figure.

in the same cluster have the same color: either black or white. At each time step, we first select two clusters with color sets (black, black), (black, white) or (white, white) having probabilities $1/(1+2p)$, $p/(1+2p)$, and $p/(1+2p)$, respectively, where p is a model parameter in the range $0 < p \leq 1$. Then, two nodes – one from each cluster – are selected randomly and connected, which causes the two clusters to merge. If the two selected clusters are the same, two distinct nodes from that cluster are connected.

The colors of all nodes in the resulting merged cluster are updated according to the following rule: if the colors of the two clusters are the same, there is no change. However, if the colors are different, then the colors of all nodes in the smaller cluster are changed to that of the larger cluster. This change may represent opinion formation following the so-called majority rule. If the sizes of both clusters are the same, but with different colors, then either color is picked with equal probability. We numerically show that if $0 < p < 1$, the PT is discontinuous and takes place at a finite threshold $t_c < 1$, and if $p = 1$, $t_c = 1$ (Fig. 2(a)). We note that if $0 < p < 1$, the symmetry between different species in the dynamic rule is broken; if $p = 1$, the symmetry is preserved.

The dynamic rule, particularly in the process of updating the color of nodes, can be modified in several ways. Nevertheless, the overall behavior of the DPT does not change significantly. To facilitate an analytic solution, we modify the dynamic rule as follows: When the colors of the two selected clusters are different, we take black regardless of cluster size, i.e., without following the majority rule. This modification enables us to set up a coupled Smoluchowski coagulation equation, and subsequently, to analytically understand the evolution of a large cluster.

Let $n_{0s}(t)$ and $n_{1s}(t)$ be the numbers of s -size black and white clusters per node, respectively, at time step t . The rate equations of the two quantities are written as

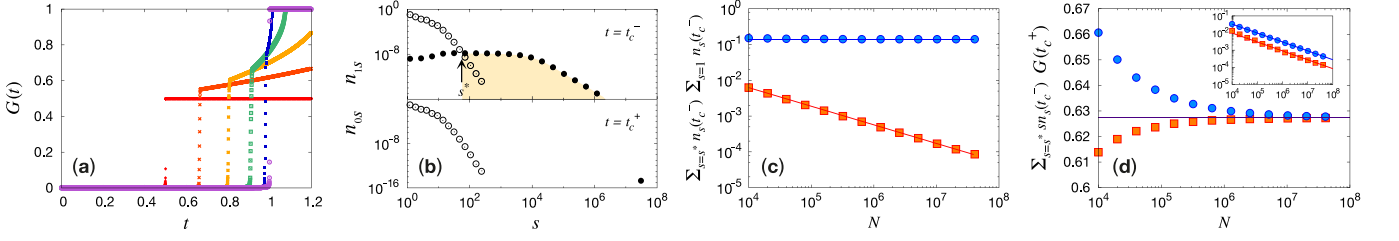


FIG. 2. (Color online) (a) Plot of $G(t)$ vs t of the TCA model for various values of p for a system size of $N = 10^5$. From left to right, $p = 0, 0.2, 0.4, 0.6, 0.8$ and 1.0 . (b) The cluster size distributions of black clusters n_{0s} (\bullet) and white clusters n_{1s} (\circ) at t_c^- (upper panel) and t_c^+ (lower panel) for $N = 2^{12} \times 10^4$. (c) Plot of $\sum_{s=s^*}^{\infty} n_s(t_c^-)$ (\square) and $\sum_{s=1}^{\infty} n_s(t_c^-)$ (\circ) vs N . (d) Plot of $\sum_{s=s^*}^{\infty} sn_s(t_c^-)$ (\square) and $G(t_c^+)$ (\circ) vs N . The two data sets converge to the value $y_0 \approx 0.63$. Inset: plot of $y_0 - \sum_{s=s^*}^{\infty} sn_s(t_c^-)$ (\square) and $G(t_c^+) - y_0$ (\circ) vs N , respectively. The slopes of the guidelines for (\square) in (c) and the inset of (d) are equal to -0.52 . The data sets for (b), (c) and (d) are obtained for $p = 0.5$.

$$\frac{dn_{0s}}{dt} = \frac{1}{1+2p} \left(\sum_{i=1, j=1}^{\infty} \frac{n_{0i}}{c_0} \frac{n_{0j}}{c_0} \delta_{i+j, s} - 2 \frac{n_{0s}}{c_0} \right) + \frac{p}{1+2p} \left(\sum_{i=1, j=1}^{\infty} \frac{n_{0i}}{c_0} \frac{n_{1j}}{c_1} \delta_{i+j, s} - \frac{n_{0s}}{c_0} \right), \quad (1)$$

$$\frac{dn_{1s}}{dt} = \frac{p}{1+2p} \left(\sum_{i=1, j=1}^{\infty} \frac{n_{1i}}{c_1} \frac{n_{1j}}{c_1} \delta_{i+j, s} - 2 \frac{n_{1s}}{c_1} \right) - \frac{p}{1+2p} \frac{n_{1s}}{c_1}, \quad (2)$$

where $c_0 = \sum_{s=1}^{\infty} n_{0s}(t)$ and $c_1 = \sum_{s=1}^{\infty} n_{1s}(t)$ are the number of finite black and white clusters per node at time t in the system, respectively. Next, we define the generating functions $f(z, t) = \sum_{s=1}^{\infty} n_{0s}(t)z^s$ and $g(z, t) = \sum_{s=1}^{\infty} n_{1s}(t)z^s$, where the summation runs over finite clusters. As a result, the rate equations (1) and (2) are changed to

$$\frac{df(z, t)}{dt} = \frac{1}{1+2p} \left(\frac{f^2}{c_0^2} - \frac{2f}{c_0} \right) + \frac{p}{1+2p} \left(\frac{fg}{c_0 c_1} - \frac{f}{c_0} \right), \quad (3)$$

$$\frac{dg(z, t)}{dt} = \frac{p}{1+2p} \left(\frac{g^2}{c_1^2} - \frac{2g}{c_1} \right) - \frac{p}{1+2p} \frac{g}{c_1}. \quad (4)$$

Using $c_0(t) = f(1, t)$ and $c_1(t) = g(1, t)$, we obtain that $c_0(t) = 1/2 - t/(1+2p)$ and $c_1(t) = 1/2 - 2pt/(1+2p)$. When $0 < p < 0.5$, the percolation threshold can be obtained by setting $c_0(t_c) = 0$ but $c_1(t_c) > 0$, because $c_0(t)$ decreases more rapidly than $c_1(t)$. Thus, $t_c = 1/2 + p$ and a large black cluster emerges at t_c . The size of the jump in the order parameter at t_c can be obtained using the formula $\Delta G = 1 - f'(1, t_c) - g'(1, t_c)$, which reduces to $\Delta G = 1 - g'(1, t_c)$, because $f'(1, t_c) = 0$. Thus, the jump in the order parameter is determined as $\Delta G = 1 -$

$\sqrt{1-2p}/2$. The PT is discontinuous at a finite threshold $t_c < 1$ and $\Delta G < 1$ (type-II DPT).

When $p \geq 0.5$, because $c_1(t)$ decreases more rapidly than $c_0(t)$, the percolation threshold can be obtained using $c_1(t_c) = 0$ and $c_0(t_c) > 0$. Thus, $t_c = \frac{1}{2} + \frac{1}{4p}$. The size of the jump in the order parameter can be obtained using the formula $\Delta G = 1 - f'(1, t_c)$. However, $f'(1, t_c) = 1$ and $f'(1, t) = 1$ even for $t < 1$. Thus $\Delta G = 0$ for $t < 1$. When $t > 1$, $f'(1, t) = 0$. Thus, the order parameter behaves as $\Delta G = 1$ for $t > 1$, and the threshold $t_c = 1$ (type-I DPT). These analytic results are checked numerically in Appendix A.

Here we test the necessary conditions for the TCA model and understand the origin of the type-II DPT. For this purpose, we plot the cluster size distribution for the TCA model immediately before and after the transition point in Fig.2(b). At t_c^- , the size distributions of the white and the black clusters decay exponentially in the asymptotic region. However, the size distribution of the black clusters is extended to a larger region due to the symmetry-breaking properties of the dynamic rule. The nodes belong to the extended (shaded) region corresponds to the powder keg referred in previous studies [9, 10, 13]. The combined cluster size distribution exhibits crossover behavior from the region primarily composed of white clusters to that primarily composed of black clusters across a characteristic size, which we denote as s^* . This segregation is induced by the symmetry breaking dynamic rule: The merging process between black clusters takes place with a higher probability than those between other types of clusters. Thus, they grow more rapidly and belong to the region $s > s^*$. At t_c^+ , when the drastically increasing order parameter $G(t)$ changes to a gradually increasing $G(t)$, the cluster size distribution is shown in the lower panel of Fig.2(b). The difference between the two figures shows that during the interval $t_c^+ - t_c^-$, almost all black clusters aggregate to form a large cluster, and a small number of white clusters merge with large-sized black clusters as black clusters. These microscopic understanding of the mechanism of a type-II DPT is schematically illustrated in Fig.3. Such origin can be also observed in other models such as the

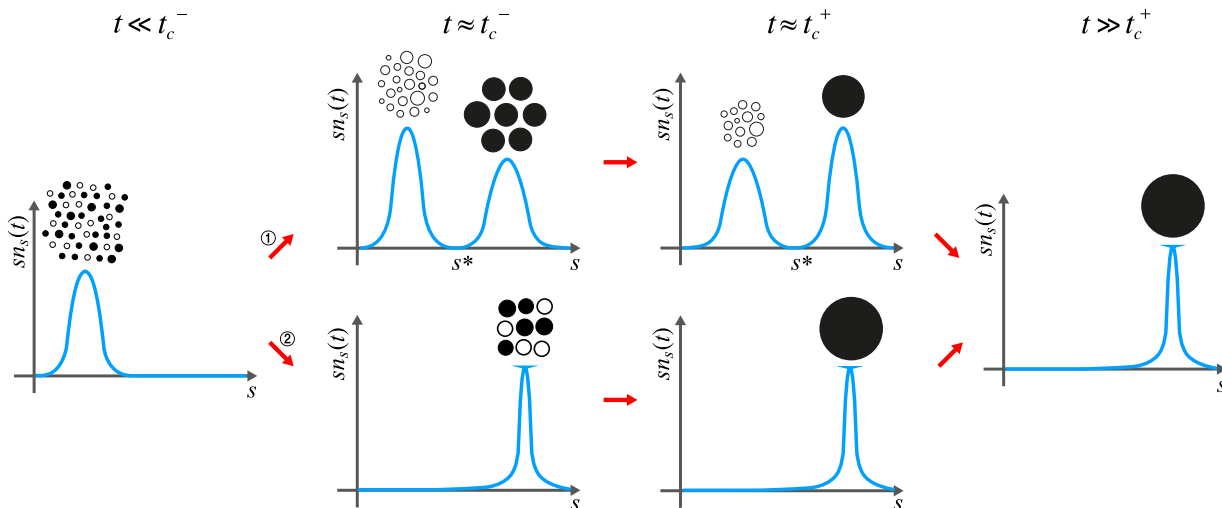


FIG. 3. (Color online) Schematic illustration of the formation of a type-I and II DPT in CM processes through ① upper pathway and ② lower pathway, respectively.

so-called the BFW model [19] and a half-restricted process model [20], which are shown in Appendix B. Based on these numerical results for the merging processes, we made the assumption stated previously when the necessary conditions were set up.

We confirm the necessary conditions numerically that the number of clusters of size $s > s^*$ at t_c^- is sub-extensive as the condition I-i). The total number of clusters over the entire range of s is, however, extensive to N as the condition I-ii) (Fig.2(c)), which is needed for a gradual increase of the order parameter beyond t_c^+ . Next, we measure the number of nodes belonging to the clusters of sizes $s > s^*$, finding that the order parameter converges to a finite value $r \approx 0.63 < 1$ as the system size is increased. The nodes belonging to this region become the elements of a macroscopic-scale giant cluster as can be seen for large N cases (Fig. 2(d)). Numerical testing for the necessary conditions is performed for other models such as the so-called BFW model [19], the half-restricted process model [20], and the ordinary percolation model in a hierarchical network with long-range connection [21]. The details are presented in Appendix A.

We remark that the origin of the type-II DPT in CM processes is different from that of the DPTs driven by the cascading-failure dynamics in interdependent networks [5] or in the k -core percolation model [23]. The cluster size distribution at t_c^- for the latter case does not look similarly to the ones of the former case. Thus, the necessary conditions we studied cannot be applied to the latter case. Meanwhile, when a type-II DPT is induced by the hierarchical structure as in [21], even though our necessary conditions were found to be valid, it is not manifest yet if the DPT is originated from symmetric breaking dynamics.

In summary, we have investigated the origins of the two types of DPT in CM processes, and derived the necessary conditions for them. We also introduced an analytically

solvable model in which two species of clusters evolve through the CM processes under symmetry-breaking rule and showed that this symmetry-breaking dynamics is observed in various type-II DPT models. We anticipate that our result can be used to understand the origin of type-II discontinuous transitions for synchronization [24] and epidemic spreading [26] models.

ACKNOWLEDGMENTS

This work was supported by the NRF grants (Grant No.2010-0015066) and the Global Frontier Program (YSC).

APPENDIX

A. Numerical testing of the necessary condition for diverse models

We check the necessary conditions for various models. Detailed statements on whether the necessary conditions are fulfilled or not are presented in the caption of each figure.

A.1. For models that show type-II discontinuous percolation transitions

Numerical testings of the necessary condition for the solvable TCA model (Fig. 4), the BFW model (Fig. 5), percolation model on hierarchical lattice (Fig. 6) and The half-restricted process model (Fig. 7) are plotted.

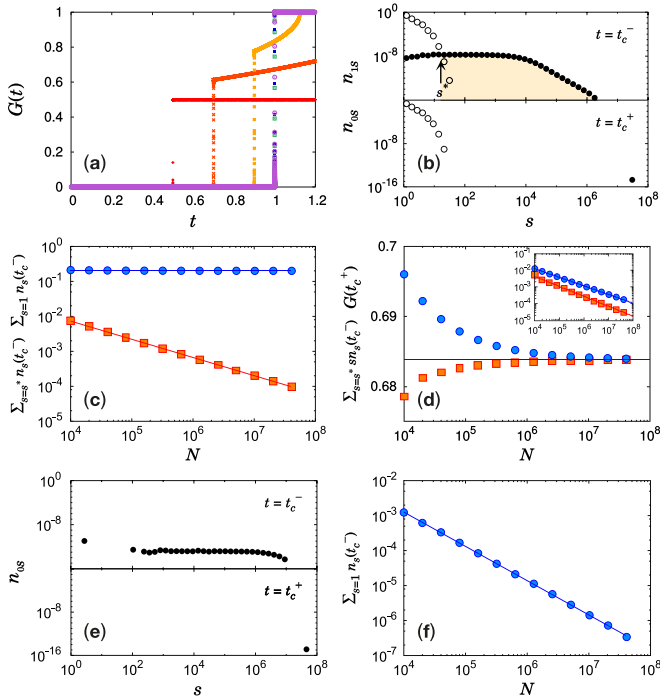


FIG. 4. (Color online) **The solvable TCA model.** (a) Plot of $G(t)$ vs t for $p = 0, 0.2, 0.4, 0.6, 0.8$ and 1.0 from left to right for a fixed system size $N = 2^{12} \times 10^4$. As p is increased, t_c is delayed. $G(t)$ exhibits a type-I percolation transition at $t_c = 1$ for $p = 0.6, 0.8$ and 1.0 . For $p = 0$, PT is also type-I, in which single-species merging dynamics takes place. (b) Plot of the size distributions of black clusters n_{0s} (●) and white clusters n_{1s} (○) for $p = 0.3$ and $N = 2^{12} \times 10^4$. Large black clusters and small white clusters coexist at t_c^- . Here, s^* denotes the crossing point of $n_{0s}(t_c^-)$ and $n_{1s}(t_c^-)$. As shown in the lower panel, all black clusters and some white clusters merge during $\Delta t = t_c^+ - t_c^-$, and consequently a large black cluster forms at t_c^+ . (c) Plot of $\sum_{s=s^*}^{\infty} n_s(t_c^-)$ (□) and $\sum_{s=1}^{\infty} n_s(t_c^-)$ (○) vs N . The slopes of the guidelines are 0 for (○) and -0.52 (□). (d) Plot of $\sum_{s=s^*}^{\infty} s n_s(t_c^-)$ (□) and $G(t_c^+)$ (○) vs N . The two data sets converge to the value $y_0 \approx 0.68$. Inset: plot of $y_0 - \sum_{s=s^*}^{\infty} s n_s(t_c^-)$ (□) and $G(t_c^+) - y_0$ (○) vs N . The slopes of the guidelines are -0.52 and -0.60 from the top. The dataset for (b-d) were obtained for $p = 0.3$. (e) Plot of the size distribution of black clusters n_{0s} (●) for $p = 1.0$ (type-I DPT case) and $N = 2^{12} \times 10^4$. In this case, only black clusters are left at t_c^- . As shown in the lower panel, all the black clusters merge during $\Delta t = t_c^+ - t_c^-$, and consequently a large black cluster of size N forms at t_c^+ . (f) We measure $\sum_{s=1}^{\infty} n_s(t_c^-)$ as a function of N for $p = 1.0$. $\sum_{s=1}^{\infty} n_s(t_c^-)$ decreases to 0 as $\sim N^{-0.98}$, which implies that the case of $p = 1.0$ satisfies the necessary condition for type-I DPT.

A.2. For a model that shows a type-I discontinuous percolation transition

Numerical testing of the necessary condition for the gaussian model (Fig. 8) is plotted.

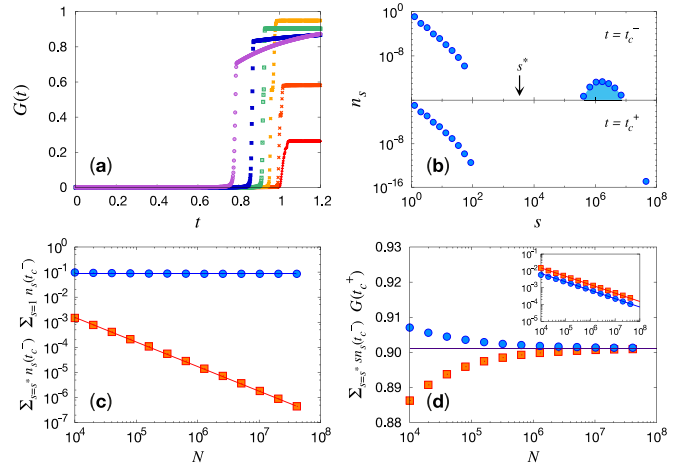


FIG. 5. (Color online) **The BFW model.** (a) Plot of $G(t)$ vs t for $\alpha = 0.2, 0.4, 0.6, 0.7, 0.8$ and 0.9 from right to left for a system size of $N = 10^5$, where α is a control parameter given in the model. (b) Plot of $n_s(t)$ vs s for $\alpha = 0.7$ and $N = 2^{12} \times 10^4$. Large and small clusters coexist at t_c^- shown in the upper panel. s^* can be naturally chosen as a point between the regions of small and large clusters. As shown in the lower panel, all large clusters merge during the interval $\Delta = t_c^+ - t_c^-$, and consequently form a large cluster. (c) $\sum_{s=1}^{\infty} n_s(t_c^-)$ (○) is independent of N and $\sum_{s=s^*}^{\infty} n_s(t_c^-)$ (□) decreases to 0 as the system size diverges. The exponent is about 0.98. (d) Plot of $G(t_c^+)$ (○) and $\sum_{s=s^*}^{\infty} s n_s(t_c^-)$ (□) seem to converge to the same value 0.90, indicated by the solid line. Inset: Plots of $G(t_c^+) - 0.90$ (○) and $0.90 - \sum_{s=s^*}^{\infty} s n_s(t_c^-)$ (□) vs N . Both quantities decay in a power-law manner with the exponent value -0.50 as shown in the Inset. The dataset for (c) and (d) were obtained for $\alpha = 0.7$.

A.3. For a model that shows a continuous percolation transition

Numerical testing of the necessary condition for the Product rule (Fig. 9) is plotted.

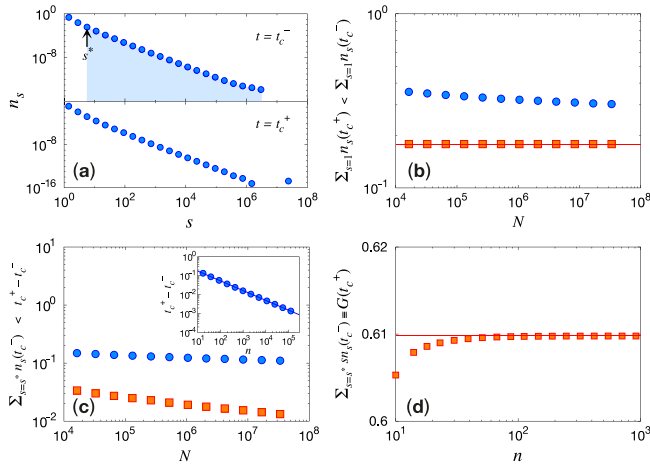


FIG. 6. (Color online) **Percolation model on hierarchical lattice with long-range connections.** (a) Plots of $n_s(t_c^-)$ and $n_s(t_c^+)$ vs s for $N = 2^{25}$ in the upper and the lower panel, respectively. In this model, since $n_s(t_c^-)$ decays monotonically, we cannot determine s^* naturally as taken in the previous cases. However, we take s^* through the relation $\sum_{s=s^*}^{\infty} sn_s(t_c^-) \equiv G(t_c^+)$, where $t_c^+ = 1$. (b) We measure $\sum_{s=1}^{\infty} n_s(t_c^+)$ (\square) and $\sum_{s=1}^{\infty} n_s(t_c^-)$ (\circ). We find that $\sum_{s=1}^{\infty} n_s(t_c^+)$ is independent of N , and thus $\lim_{N \rightarrow \infty} \sum_{s=1}^{\infty} n_s(t_c^-) \sim O(1)$ by the relation $\sum_{s=1}^{\infty} n_s(t_c^-) > \sum_{s=1}^{\infty} n_s(t_c^+)$. (c) We measure $\sum_{s=s^*}^{\infty} n_s(t_c^-)$ (\square) and $t_c^+ - t_c^-$ (\circ). By the definition of s^* , $\sum_{s=s^*}^{\infty} n_s(t_c^-) < t_c^+ - t_c^- \rightarrow 0$ satisfies and thus, $\sum_{s=s^*}^{\infty} n_s(t_c^-) \rightarrow 0$. Inset: $t_c^+ - t_c^-$ decreases to 0 as $\sim n^{-0.51}$, where $n = \log_2 N$. (d) Finally, we measure the $\sum_{s=s^*}^{\infty} sn_s(t_c^-) \equiv G(t_c^+)$ as a function of n and find that $\sum_{s=s^*}^{\infty} sn_s(t_c^-)$ converges to 0.61, which is equivalent to the analytic result.

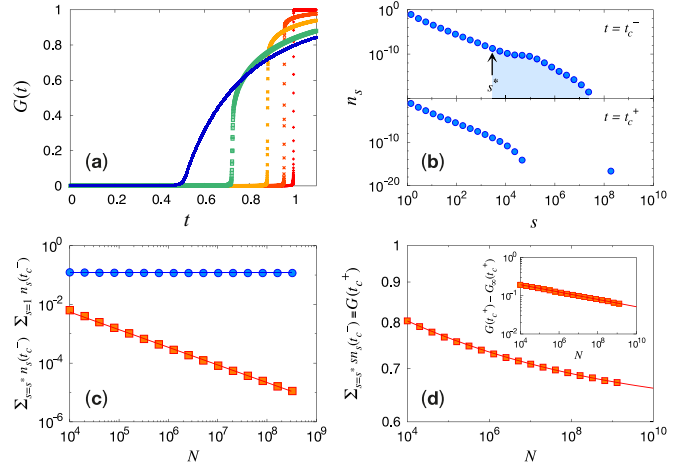


FIG. 7. (Color online) **Half-restricted process model** (a) Plot of $G(t)$ vs t for various values of $d = 0.2, 0.4, 0.6, 0.8$ and 1.0 for a system size of $N = 10^5$ from right to left, where d is a control parameter given in the model. (b) Plot of $n_s(t_c^-)$ vs s for $d = 0.5$ and $N = 2^{15} \times 10^4$ in the upper panel. Here, again s^* was determined using $\sum_{s=s^*}^{\infty} sn_s(t_c^-) \equiv G(t_c^+)$. After $\Delta t = t_c^+ - t_c^-$, a large cluster is formed as shown in the lower panel. (c) We plot $\sum_{s=1}^{\infty} n_s(t_c^-)$ (\circ) vs N to confirm its independency of N . We also confirm that $\sum_{s=s^*}^{\infty} n_s(t_c^-)$ (\square) decreases to 0 as $\sim N^{-0.60}$. (d) $\sum_{s=s^*}^{\infty} sn_s(t_c^-) \equiv G_N(t_c^+)$ decreases with respect to N , but it seems to be saturated asymptotically. We estimated the saturated value by extrapolating the data to be $G_{\infty}(t_c^+) \approx 0.61$. Inset: It shows that $G_N(t_c^+) - G_{\infty}(t_c^+) \sim N^{-0.10}$. Numerical data for (c) and (d) were obtained for $d = 0.5$.

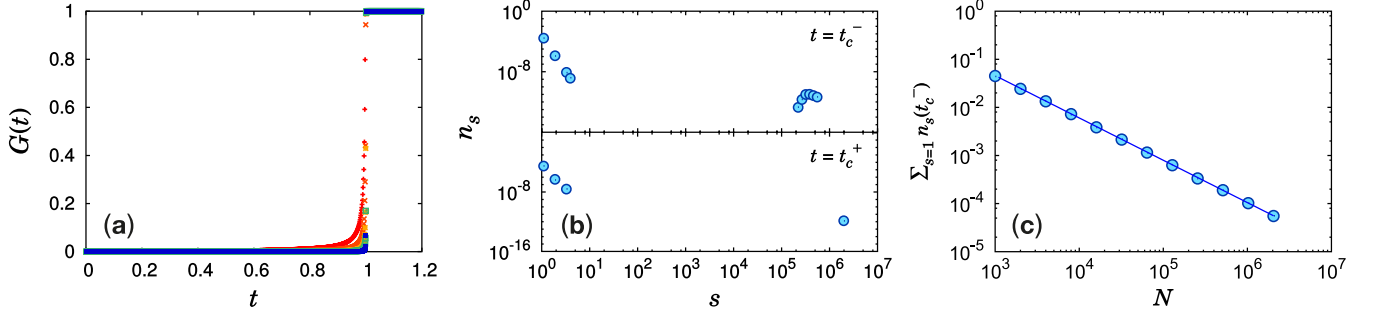


FIG. 8. (Color online) **Gaussian model** (a) Plot of $G(t)$ vs t for $N = 10^5$ with parameter values $\alpha = 10^{-4}, 10^{-3}, 10^{-2}, 10^{-1}$ and 1 from the left, where α is a control parameter given in the model. (b) Plot of $n_s(t_c^-)$ vs s for $N = 2^{11} \times 10^3$ and $\alpha = 10^{-2}$ in the upper plot. Large and small clusters coexist at t_c^- as shown in the upper panel. As shown in the lower panel, all large clusters merge during the time interval $\Delta t = t_c^+ - t_c^-$, and consequently form a large cluster. (c) Plot of $\sum_{s=1}^{\infty} n_s(t_c^-)$ vs N for $\alpha = 10^{-2}$. It decays in a power law manner as $N^{-0.88}$, which fulfills the necessary condition for type-I DPT.

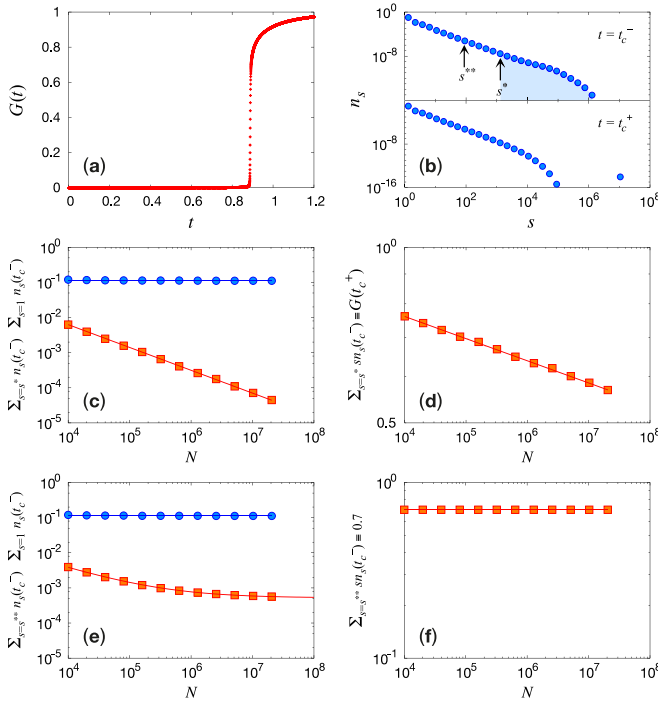


FIG. 9. (Color online) **Product rule model**. (a) Plot of $G(t)$ vs t for $N = 2^4 \times 10^4$. (b) Plot of $n_s(t_c^-)$ vs s for $N = 2^{12} \times 10^4$ in the upper panel. For this model, we were not able to determine s^* easily as the case of the TCA model. s^* and s^{**} are determined using $\sum_{s=s^*}^{\infty} sn_s(t_c^-) \equiv G(t_c^+)$ and taking $\sum_{s=s^{**}}^{\infty} sn_s(t_c^-) \equiv 0.7$, respectively. After a transient time $\Delta t = t_c^+ - t_c^-$, a large component is formed as shown in the lower plot. (c) $\sum_{s=1}^{\infty} n_s(t_c^-)$ is independent of system size and $\sum_{s=s^*}^{\infty} n_s(t_c^-)$ decreases to 0 as $\sim N^{-0.71}$. (d) $\sum_{s=s^*}^{\infty} sn_s(t_c^-) \equiv G(t_c^+)$ decreases to 0 as $N^{-0.05}$. (e) $\sum_{s=1}^{\infty} n_s(t_c^-)$ is independent of system size and $\sum_{s=s^{**}}^{\infty} n_s(t_c^-)$ decreases and approaches a certain finite value. (f) $\sum_{s=s^{**}}^{\infty} sn_s(t_c^-)$ is independent of N . As a result, this model does not fulfill both necessary conditions for type-I and II DPT and the type of the percolation transition becomes continuous in the thermodynamic limit.

B. How the symmetry breaking dynamics leads to a type-II DPT?

We introduce the necessary conditions for each species of clusters and check how a type-II DPT is induced by the symmetry breaking dynamics in the following models.

B.1. The necessary conditions for symmetry breaking dynamics

As clusters merging proceeds, clusters are segregated into two types 0 and 1 satisfying the following conditions.

- (i) $\sum_{s=1}^{s^*} n_{0s}(t_c^-) \rightarrow 0$ and $\sum_{s=s^*}^{\infty} n_{0s}(t_c^-) \rightarrow 0$. These conditions lead to an abrupt PT, driven by merging clusters of type 0 themselves.
- (ii) $\sum_{s=1}^{s^*} sn_{0s}(t_c^-) \rightarrow 0$ and $\sum_{s=s^*}^{\infty} sn_{0s}(t_c^-) = r$ ($0 < r < 1$). These conditions lead to a type-II DPT in which the order parameter is increased as much as r by merging clusters of type 0 themselves.
- (iii) $\sum_{s=1}^{s^*} n_{1s}(t_c^-) \sim O(1)$ and $\sum_{s=s^*}^{\infty} n_{1s}(t_c^-) \rightarrow 0$. These conditions lead to a gradual growth of a giant cluster by merging clusters of type 1 after the abrupt transition. Without these conditions, the giant cluster could not grow continuously after the discontinuous percolation transition.
- (iv) $\sum_{s=1}^{s^*} sn_{1s}(t_c^-) = 1 - r$. This is the complement to the condition (ii).

Combining the above necessary conditions, the following necessary conditions are obtained for a type-II DPT.

- I-i) $\sum_{s=s^*}^{\infty} n_s(t_c^-) \rightarrow 0$, I-ii) $\sum_{s=1}^{\infty} n_s(t_c^-) \sim O(1)$, and
- I-iii) $\sum_{s=s^*}^{\infty} sn_s(t_c^-) = r$ ($0 < r < 1$).

B.2. Numerical testing of the necessary conditions for each species for several models showing type-II DPTs

Numerical testings of the necessary condition for the TCA model in the main text (Fig. 10), the half-restricted process model (Fig. 11) and the BFW model (Fig. 12) are plotted.

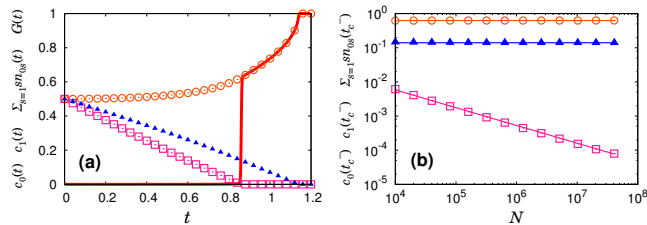


FIG. 10. (Color online) **TCA model.** (a) For the TCA model, plots of the total number of clusters of type 0 divided by N denoted as $c_0(t) = \sum_{s=1}^{\infty} n_{0s}(t)$ (\square), that of 1-type denoted as $c_1(t) = \sum_{s=1}^{\infty} n_{1s}(t)$ (\blacktriangle), $\sum_{s=1}^{\infty} sn_{0s}(t)$ (\circ), and the size of the giant cluster divided by N denoted as $G(t)$ (Solid line and curve) as a function of time t . Those quantities satisfy the necessary conditions. (b) Plots of $c_0(t_c^-)$, $c_1(t_c^-)$ and $\sum_{s=1}^{\infty} sn_{0s}(t_c^-)$ as a function of system size N . They behave as $c_0(t_c^-) \sim O(N^{\alpha-1})$ with $\alpha < 1$, $c_1(t_c^-) \sim O(1)$, $\sum_{s=1}^{\infty} sn_{0s}(t_c^-) \sim O(1)$, respectively.

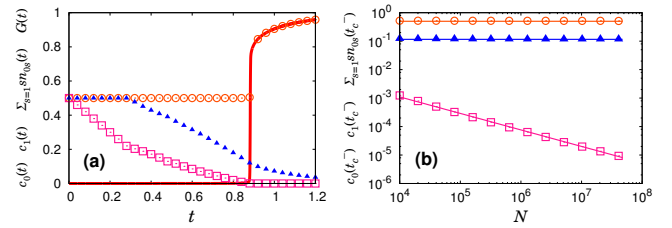


FIG. 11. (Color online) **Half-restricted process model.** (a) Similar plots for the half-restricted process model. The three quantities behave similarly as those for the TCA model. The half-restricted process model is defined as follows: At each step, we choose one node randomly from all nodes, and another node randomly from a restricted set A of nodes. The set A is defined via the formula $\sum_{s=1}^{s^*} sn_s(t) = d$, where s^* is the size of the largest cluster in the set A. That is, the number of nodes belonging to the set A is dN , where we take $d = 0.5$. The set B is defined as a set containing the rest clusters in the system. The clusters of type 0 are defined as the ones in the set B, and the clusters of type 1 are the ones in the set A. (b) Plots of $c_0(t_c^-)$, $c_1(t_c^-)$ and $\sum_{s=1}^{\infty} sn_{0s}(t_c^-)$ as a function of system size N . They behave as $c_0(t_c^-) \sim O(N^{\alpha-1})$ with $\alpha < 1$, $c_1(t_c^-) \sim O(1)$, $\sum_{s=1}^{\infty} sn_{0s}(t_c^-) \sim O(1)$, respectively.

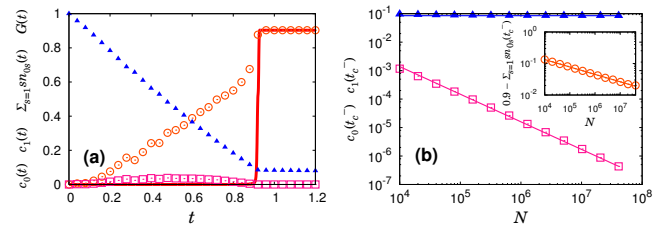


FIG. 12. (Color online) **BFW model.** (a) Similar plots for the so-called BFW model for a model parameter value $\alpha = 0.7$. In this model, the three quantities $c_0(t)$, $c_1(t)$ and $\sum_{s=1}^{\infty} sn_{0s}(t)$, behave similarly as those for the half-restricted process model. The clusters of type 0 are defined as the ones that are suppressed to grow (i.e. the clusters larger than half of the cap size given in this model). (b) Plots of $c_0(t_c^-)$, $c_1(t_c^-)$ and $\sum_{s=1}^{\infty} sn_{0s}(t_c^-)$ as a function of system size N . They behave as $c_0(t_c^-) \sim O(N^{\alpha-1})$ with $\alpha < 1$, $c_1(t_c^-) \sim O(1)$, and $\sum_{s=1}^{\infty} sn_{0s}(t_c^-) \sim O(1)$, respectively.

- [1] D. Stauffer and A. Aharony, *Introduction to Percolation Theory* (Taylor and Francis, London, 1994).
- [2] P. J. Flory, *J. Am. Chem. Soc.* **63**, 3083 (1941).
- [3] G. Grassberger, *Math. Biosci.* **63**, 157 (1983).
- [4] D. Achlioptas, R. M. D'Souza, and J. Spencer, *Science* **323**, 1453-1455 (2009).
- [5] S. V. Buldyrev, R. Parshani, G. Paul, H. E. Stanley, and S. Havlin, *Nature* **464**, 1025-1028 (2010).
- [6] S.-W. Son, G. Bizhani, C. Christensen, P. Grassberger, and M. Paczuski, *Europhys. Lett.* **97**, 16006 (2012).
- [7] R. M. Ziff, *Phys. Rev. Lett.* **103**, 045701 (2009).
- [8] Y. S. Cho, J. S. Kim, J. Park, B. Kahng, and D. Kim, *Phys. Rev. Lett.* **103**, 135702 (2009).
- [9] E. J. Friedman and A. S. Landsberg, *Phys. Rev. Lett.* **103**, 255701 (2009).
- [10] H. Hooyberghe and B. VanSchaeybroeck, *Phys. Rev. E* **83**, 032101 (2011).
- [11] R. M. D'Souza and M. Mitzenmacher, *Phys. Rev. Lett.* **104**, 195702 (2010).
- [12] R. A. da Costa, S. N. Dorogovtsev, A. V. Goltsev, and J. F. F. Mendes, *Phys. Rev. Lett.* **105**, 255701 (2010).
- [13] O. Riordan and L. Warnke, *Science* **333**, 322-324 (2011).
- [14] H. K. Lee, B. J. Kim, and H. Park, *Phys. Rev. E* **84**, 020101(R) (2011).
- [15] J. Nagler, A. Levina, and M. Timme, *Nat. Phys.* **7**, 265-270 (2011).

- [16] Y. S. Cho, S. Hwang, H. J. Herrmann, and B. Kahng, *Science* **339**, 1185-1187 (2013).
- [17] Y. S. Cho, B. Kahng, and D. Kim, *Phys. Rev. E* **81**, 030103(R) (2010).
- [18] N. A. M. Araújo and H. J. Herrmann, *Phys. Rev. Lett.* **105**, 035701 (2010).
- [19] T. Bohman, A. Frieze, and N. C. Wormald, *Random Struct. Algorithms* **25**, 432-449 (2004).
- [20] K. Panagiotou, R. Spöhel, A. Steger, and H. Thomas, *Elec. Notes in Discrete Math.* **38**, 699-704 (2011).
- [21] S. Boettcher, V. Singh, and R. M. Ziff, *Nat. Commun.* **3**, 787 (2012).
- [22] J. Chalupa, P.L. Leath, and G.R. Reich, *J. Phys. C* **12**, L31 (1981); P.M. Kogut and P.L. Leath, *J. Phys. C* **14**, 3187 (1981).
- [23] S. N. Dorogovtsev, A. V. Goltsev, and J. F. F. Mendes, *Phys. Rev. Lett.* **96**, 040601 (2006).
- [24] J. Gómez-Gardeñes, S. Gómez, A. Arenas, and Y. Moreno, *Phys. Rev. Lett.* **106**, 128701 (2011).
- [25] P. Echenique, J. Gómez-Gardeñes, and Y. Moreno, *EPL* **71**, 325-331 (2005).
- [26] H.-K. Janssen, M. Müller and O. Stenull, *Phys. Rev. E* **70**, 026114 (2004).